

Radiographic imaging of the thorax in newborn calves with anorectal anomalies

Mohammed A.H. Abdelhakiem*, Aya Hamdy Mustafa

Department of Surgery, Anesthesiology and Radiology, Faculty of Veterinary Medicine, Assiut University, Assiut, 71526, Egypt.

ARTICLE INFO

Received: 04 December 2024

Accepted: 03 January 2025

*Correspondence:

Corresponding author: Mohammed A.H. Abdelhakiem
E-mail address: hamdysurgery@aun.edu.eg

Keywords:

Newborn calves, Anorectal anomalies, Radiography, Thorax

ABSTRACT

The present study aimed to understand the radiographic anatomy of the thorax in newborn calves and to investigate the effect of anorectal anomalies on respiratory and cardiovascular structures. The study included thirty newborn calves. All were male except four. Their ages ranged from 1 to 5 days. Upon arrival at the Veterinary Teaching Hospital (VTH), the animals underwent clinical and radiographic examinations. The calves were divided into two groups: the anorectal group (n=19) and the non-anorectal group (n=11). The radiographic examination focused on both the abdomen and thorax in the first group, while the second group was assessed primarily for other conditions, such as mandibular or limb fractures, alongside thoracic evaluation. Two lateral radiographic views of the thorax were obtained for each animal. Key measurements were taken, which included the cranial pulmonary blood vessels, vertebral heart score (VHS), diameter of the caudal vena cava (CVC), diameter of the aorta, tracheal diameter, thoracic inlet, thoracic length, and thoracic axis. The heart size was evaluated using a new method that divided the sum of cardiac long axis (CLA), cardiac short axis (CSA) by the length of the thoracic inlet. The results indicated that there were no significant changes in clinical examination findings between the two groups, except for an increased respiratory rate in the anorectal group. Radiographic findings showed no significant differences between the right and left lateral views within each group. However, clear differences were observed between the anorectal and non-anorectal groups in terms of CLA, CSA, VHS, thoracic length, and thoracic axis ($P < 0.05$). There was no significant change in heart size according to the new method between the two groups. In conclusion, radiography is a valuable tool for understanding the thoracic anatomy of newborn calves. Anorectal anomalies lead to significant changes in some thoracic structures due to abdominal distension and pressure on the diaphragm. Additionally, different methods for assessing cardiac size are unreliable and should not be solely relied upon for definitive conclusions about heart size.

Introduction

The thorax comprises numerous structures related to the respiratory and cardiovascular systems. Detailed knowledge of these structures provides insight into changes in these systems. Newborn calves are commonly susceptible to respiratory issues with or without neonatal diarrhea, yet few studies have investigated the radiographic features of the thoracic cavity. In addition, previous studies focused on the radiographic evaluation of the thorax in dogs, cats, and horses, but not in bovines. Radiography is an essential tool used in veterinary clinics and hospitals to screen the thorax of animals. Radiography can effectively detect thoracic lesions in calves (Farrow, 1999). Radiography and other diagnostic tools are valuable in providing a detailed view of the thoracic cavity in animals. The boundaries of the thorax can be thoroughly examined using radiography. The thoracic vertebrae (number, shape, and anomalies), sternum (number of sternebrae, shape of sternum), and ribs (fractures) are easily detected by radiography. The continuity of the diaphragm can also be evaluated using radiography (Thrall and Robertson, 2016; Abdelhakiem, 2018; Abdelhakiem *et al.*, 2020). Radiography provides a valuable way to assess lung tissue and identify different lung patterns. By obtaining different radiographic views, it is possible to trace and examine the heart, along with major blood vessels such as the caudal vena cava, pulmonary blood vessels, and aorta. Using radiography, it is possible to detect abnormal materials in the mediastinum and pleural cavity, such as fluid and air (Carey, 1999; Abdelhakiem, 2018). Thoracic radiography can effectively detect infectious bronchopneumonia in hospitalized dairy calves. It is also capable of identifying lesions in the deep parenchyma of the lungs. Taking two views generally covers most of the lung surface area. The sensitivity of thoracic radiography for detecting pleuropneumonia in hospitalized dairy calves is 89% (Berman *et al.*, 2020).

Anorectal anomalies are structural or functional defects that appear at birth in neonatal animals in the anorectal region. It includes atresia ani, atresia recti, atresia ani et recti, and segmental aplasia of the rectum with the presence of the anal opening (Abdel-Hakiem and Aref, 2013; Abdel-

hakiem, 2020). It was reported that calves are more likely to have large intestine congenital anomalies than any other species (Kilic and Sarkerler, 2004; Abdel-Hakiem and Aref, 2013). The accumulation of meconium and gases within the intestine without being expelled may increase the intraperitoneal pressure, pushing the diaphragm forward and potentially impacting thoracic structures. We hypothesized that distended viscera caused by an obstructed exit pathway of the meconium or feces in neonates may have an impact on the cardiovascular or respiratory constituents of the thorax.

The present study was conducted to determine the effect of anorectal anomalies (absence of the ability to defecate) on the radiographic findings of the different thoracic structures in newborn calves. These results are compared to those obtained from newborn calves admitted to the hospital for causes unrelated to anorectal anomalies. The present study aimed for understanding the radiographic anatomy of the calf's thorax which is essential to detect the different thoracic lesions. A new way for measuring cardiac size used in dogs is applied in this study to evaluate heart size.

Materials and methods

Animals

The study did not require ethical approval as it is classified as a case series study. It focused on animals presented to the Animal Surgery Department at the Veterinary Teaching Hospital, Assiut University, Egypt, between January 2023 and November 2023. A complete medical history was collected from the owners, and a clinical examination was conducted on all the animals. Based on their main issues, the animals were referred for radiographic examinations (Figure 1).

The study was carried out on thirty newborn calves, with ages ranging from 1 to 5 days and weights between 40 and 60 kg. Among these calves, there were twenty-six males and four females. The animals were divided into two groups: Group A consisted of neonatal calves with ano-

rectal anomalies (n=19), while Group B included neonatal animals with conditions other than anorectal anomalies (n=11).

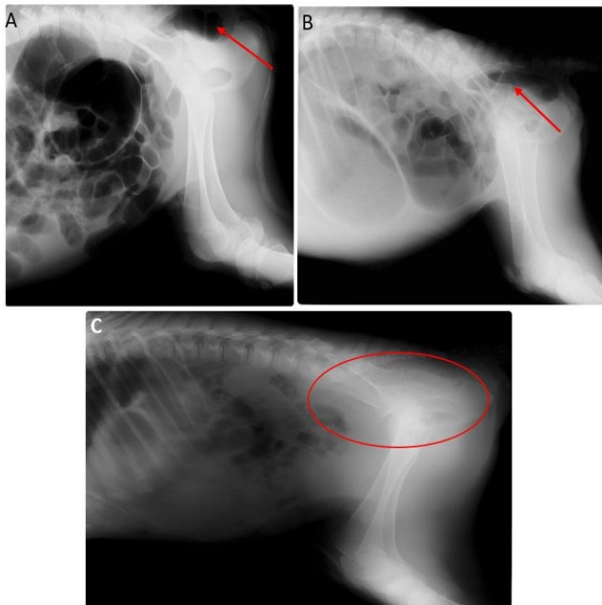


Fig. 1. Lateral radiographs of the abdomen in newborn calves with atresia ani (A&B). Notice the presence of gas in the caudal part of the GIT (rectum) which was depicted by red arrows. The figure C shows the lateral radiograph of abdomen in newborn calf with atresia recti. Notice a soft tissue density free from gases (red circle).

History and clinical examination

The calves were admitted within the first few days of their lives. Calves in Group A experienced the absence of an anal opening or defecation, along with varying degrees of abdominal distension. Animals in Group B exhibited different symptoms depending on their presenting affection. These symptoms included a protruding tongue and salivation in cases of mandibular fractures. Other calves displayed an abnormal gait or were unable to stand and walk due to fractures in their limbs. A comprehensive clinical examination was conducted for all the animals, which included assessing body temperature, heart rate, respiratory rate, and hydration status. The body temperature in the animals with anorectal anomalies was measured through the oral route (sublingual) and axillary route. Also, these routes plus the rectal route were applied in the second group to determine the accurate body temperature of calves in the first group.

Radiographic evaluation

All calves were subjected to radiographic examination using CR apparatus (Ceiling suspended tube stand: model GXR-68 DRGEM; address of factory: 213, Saneopdanji-ro, Eomo-myeon, Gimcheon-si, Gyeong-sangbuk-do, Republic of Korea; 2020& FujiFilm corporation (CR scanner), MINATO-KU, TOKYO, JAPAN; 2019). The radiographic factors were 40-45 mAs, and 50-55 Kv. The focal spot film distance was about 75-80 cm.

All the following structures were evaluated using right and left lateral views of radiographs. The vertebral heart score (VHS) was calculated by summing the long axis and short axis measurements of the heart, which were then compared to a vertebral line starting from the cranial end of the fourth thoracic vertebra (Figure 2). The measurement of the VHS was performed according to the method described by Abdelhakiem *et al.* (2020). The cardiac size is measured also according to Fernández *et al.* (2023). The summation of CLA and CSA was divided on the length of thoracic inlet (Figure 2). Additionally, the cranial pulmonary blood vessels (CPBV) were assessed to determine whether they were clear and distinct on the radiograph (Figure 3). If they were visible, their diameters were measured. The diameter of the CPBV was compared to the width of the most proximal part of the fourth rib. The diameter of the aorta was measured at its base, just above the trachea. The caudal vena cava (CVC) was

measured at the midpoint between the heart and the diaphragm (Figure 4). The ventral wall of the CVC was measured, representing the distance between the heart and the diaphragm. The tracheal diameter was measured and compared to the thoracic inlet at the same point. The axial length of the thorax from the diaphragm (ventral wall of CVC) to the thoracic inlet was estimated. The length of the thorax (from the ventral wall of the thoracic vertebrae to the dorsal wall of the sternum passing through the carina and on the same line of the cardiac length) was valued (Figure 4). The precise location of the carina, which is the tracheal bifurcation, was identified based on the thoracic vertebrae. The number of sternbrae of the sternum was counted.

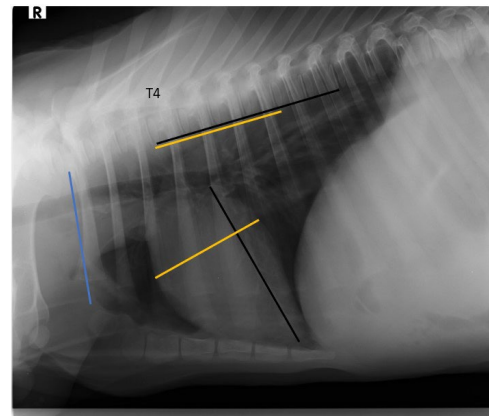


Fig. 2. Right lateral radiograph shows the calculation of the vertebral heart score (VHS) in 2 days old male calf. The black line represents the cardiac long axis (CLA), and the yellow line represents the cardiac short axis (CSA). The two lines are dissected to each other forming square angle. The calculation of the VHS started from the cranial end of the thoracic vertebral no. 4 (T4). The summation of the vertebrae which are included by the two lines results in the VHS. Black line= 6 vertebra, and yellow line= 4 vertebra. Therefore, the VHS= 6+4= 10. The blue line represents the length of thoracic inlet from ventral aspect of 1st thoracic vertebra to the dorsal aspect of the 1st sternbra (manubrium). The heart size measurement according to the Fernández method is equal (CLA+CSA)/length of thoracic inlet.

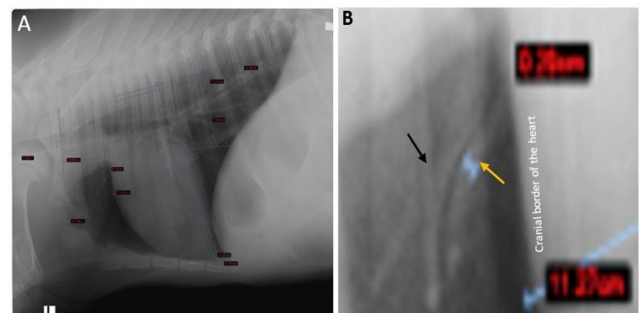


Fig. 3. Left lateral radiograph of 2 days old calf with atresia ani shows the visualization and measurement of different thoracic structures (A), and close-up of the left figure (A) displayed the magnified cranial pulmonary vessels. The width of the cranial pulmonary vein (blue H shape) which is indicated by yellow arrow. The cranial pulmonary artery is bifurcated distally (black arrow).

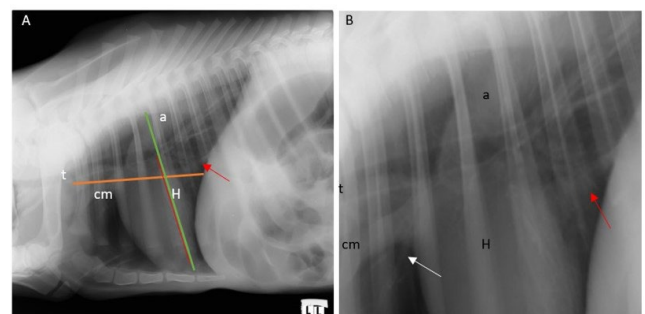


Fig. 4. left lateral radiograph of 4 days old male newborn calf with atresia ani (A) shows the cardiac silhouette (H) and main blood vessels (aorta (a), caudal vena cava (red arrow), cranial mediastinum (cm) and trachea (t)). The orange line denotes the thoracic axis from diaphragm to thoracic inlet. The green line refers to the thoracic length from the ventral aspect of the thoracic vertebrae to the dorsal aspect of the sternum. This line overlies the cardiac long axis (the red line). The right figure (B) is the zoom-out of figure A to shows the base of the heart and blood vessels. The white arrow refers to the cranial pulmonary blood vessel. Notice the decrease in diameter of CVC (1.28 cm in this case) especially if it is compared to the diameter of aorta (2.67 cm in this case). This may refer to the decrease of venous return.

Statistical analysis

The data was analyzed using SPSS software version 21 (IBM Corp., Armonk, NY, USA). The data was expressed as mean ± SEM. The Paired T-test was employed to assess the differences in measured thoracic structures recorded in both the right and left lateral views of calves with ano-rectal anomalies. Additionally, this test was also applied to data collected from calves with lesions that were not classified as ano-rectal anomalies. One-way ANOVA was utilized to compare the means of measured thoracic structures between ano-rectal anomalies and other lesions in both lateral views.

Results

The current study involved thirty newly born calves of various breeds, including both native and mixed breeds. All but four of the animals were male. A clinical examination of all calves revealed that they were generally healthy. The temperature, heart rate, and respiratory rate in the ano-rectal group were 39.06±0.09°C, 86.8±0.84 beat/min, and 23.6±1.15 breath/min, respectively, while they were in the other group 38.98±0.17°C, 83.7±1.53 beat/min, and 16.64±0.85 breath/min respectively. Significant differences were observed between the two groups only in the respiratory rate (P = 0.00). About half degree of Celsius was added to the oral route obtained body temperature and 2.5 degrees was added to the axillary route obtained body temperature.

The animals were divided into ano-rectal groups (n=19), and non-ano-rectal group (n=11). The ano-rectal group included 17 calves that had atresia ani and 2 calves suffered atresia recti. Their age ranged from 1 to 5 days (mean 2.3 days), and their weight ranged between 40 and 60 kg (mean 46.6 kg). All the animals in this group were male, except for three which were female. The animals of the other group were admitted to the VTH with affections other than the ano-rectal anomalies (n=11). These affections included fractured mandible (n=4), Arthrogryposis (n=1), umbilical eventration and intestinal prolapse (n=1), a mild degree of omphalitis without systemic disturbance (n=1), ataxia (n=1), fracture of right radius

(n=1), fracture of left radius (n=1), fracture of left metatarsal bone (n=1). Their age ranged from 1-5 days (mean= 2.45 days), and their weight ranged from 40- 55 kg (mean= 45 kg). All animals in this group were male except one animal.

Radiographic evaluation

The mean measurements of the thoracic structures observed in the left and right lateral views of the radiographs for both groups are summarized in Table 1. The statistical analysis indicated no significant changes in the measured structures on the lateral radiographic views for the ano-rectal group, except for the thoracic inlet, which showed a significant difference (P = 0.006).

In the second group, the analysis revealed significant differences between the right and left lateral radiographs for the cardiac long and short axes (CLA, CSA) and the trachea, with P-values of 0.019, 0.024, and 0.047, respectively.

Additionally, significant differences were noted in the CLA, vertebral heart score (VHS), thoracic length, thoracic axis, and the ventral wall of the caudal vena cava (CVC) on the right lateral views in both groups (P = 0.043, 0.021, 0.003, 0.02, and 0.023, respectively) as shown in Table 2.

Clear differences were also observed in the CSA, width of the fourth rib, CVC, trachea, thoracic inlet, thoracic axis, and the CLA/thoracic length ratio on the left lateral radiographic views of the two different groups (P = 0.048, 0.046, 0.032, 0.013, 0.008, 0.003, and 0.04, respectively), as detailed in Table 2.

On the right radiographic lateral view of the ano-rectal group, the cranial pulmonary vessels were visualized in all animals. The CVC was clear in 18 out of 19 cases. However, the aorta was not visible in 4 out of 19 cases. The position of the Carina varied on the radiographs, being located at the level of C4-C5 in 11 cases, C5-C6 in 6 cases, and C3-C4 in 2 cases.

On the left lateral view of the ano-rectal group, the cranial pulmonary vessels were not identifiable in three out of 19 cases. The CVC was visualized in all cases, while the aorta was visible in only 15 out of 19 cases. The carina was located at the C4-C5 level in 13 out of 19 cases, at the C5-C6

Table 1. Differences between different thoracic structures on the two lateral radiographic views in each group

Thoracic structure	RLV Ano-rectal (n=19)	LLV Ano-rectal (n=19)	RLV Others (n=11)	LLV Others (n=11)
CLA (cm)	13.57± 0.27	13.6± 0.22	14.5± 0.34*	14.21± 0.31*
CSA (cm)	9.02± 0.26	9.05± 0.30	9.69± 0.335*	10.06± 0.36*
VHS (number of vertebrae)	9.6± 0.15	9.57± 0.19	9.04± 0.174	9.13± 0.19
Pulm. Artery (cm)	0.286± 0.0197	0.23± 0.033	0.277± 0.0392	0.25± 0.03
Pulm. Vein (cm)	0.285± 0.0193	0.23± 0.032	0.2755± 0.0391	0.26± 0.032
4th rib (cm)	0.56± 0.03	0.55± 0.03	0.64± 0.04	0.65± 0.03
Ratio 1	0.55± 0.05	0.46± 0.07	0.45± 0.07	0.39± 0.05
CVC (cm)	1.5± 0.135	1.39± 0.116	1.81± 0.09	1.75± 0.105
Aorta (cm)	1.88± 0.24	1.6± 0.25	2.43± 0.27	1.996± 0.42
Ratio 2	0.5± 0.073	0.42± 0.76	0.62± 0.072	0.48± 0.102
Sternum (number of sternebrae)	6.74± 0.10	6.78± 0.10	6.64± 0.15	6.64± 0.15
Trachea (cm)	1.16± 0.053	1.14± 0.041	1.255± 0.057*	1.33± 0.06*
Thoracic inlet (cm)	10.05± 0.185*	10.33± 0.25*	10.291± 1.098	11.19± 0.33
Ratio 3	0.12± 0.004	0.10± 0.007	0.11± 0.004	0.119± 0.006
Thoracic length (cm)	18.23± 0.31	18.3± 0.37	19.915± 0.43	19.84± 0.383
Thoracic axis (cm)	15.32± 1.30	16.87± 0.64	19.772± 0.66	19.84± 0.62
Ventral wall CVC (cm)	3.39± 0.30	3.55± 0.37	4.521± 0.33	4.17± 0.34
CLA/thoracic length	0.74± 0.008	0.75± 0.009	0.73± 0.008	0.72± 0.009
Fernandez method (CLA+CSA)/TIH	2.25± 0.0423	2.2± 0.0495	2.14± 0.067	2.18± 0.0585

Data are presented as Mean±SEM. The significant difference in each group on both lateral views was superscripted by asterisk (*). CLA: cardiac long axis; CSA: cardiac short axis; VHS: vertebral heart score or scale; Pulm. Artery: pulmonary artery; pum. Vein: pulmonary vein; 4th rib: fourth rib; Ratio 1: pulm. Artery/4th rib; CVC: caudal vena cava; Ratio 2: CVC/Aorta; Ratio 3: trachea/thoracic inlet; ventral wall CVC: ventral wall of caudal vena cava; CLA/ thoracic length: cardiac long axis: thoracic length at the same point; CLA+ CSA/TIH: (cardiac long axis+ cardiac short axis)/ thoracic inlet height or length.

level in four cases, and at the C3-C4 level in two cases.

The right lateral radiographic views of the second group showed that the cranial pulmonary vessels were visible in 10 out of 11 cases. CVC was identified in all cases. The aorta was not visualized in 1 out of 11 cases. The position of the carina varied on the radiographs: it was located at the C4-C5 level in 6 out of 11 cases, at the level of mid C5 in 2 cases, at the C3-C4 level in 1 case, and at the C5-C6 level in 2 cases.

Regarding to the left lateral radiographic view of the second group, the cranial pulmonary vessels were not visible in one case. The CVC was clearly identified in all cases, while the aorta was visualized in only 9 out of 11 cases. The carina was located at the C4-C5 level in 7 out of 11 cases, at the C5-C6 level in 3 cases, and at the mid C5 level in 1 case.

Discussion

The present work aimed to determine the effect of anorectal anomalies in newly born calves on the thoracic structures. This effect was evaluated by radiography. The results of the present study revealed significant changes between the anorectal group and the other group. There was clear decrease in the cardiac long axis, VHS, thoracic length, thoracic axis, CVC and ventral wall of CVC on one or two radiographic lateral views in the group of anorectal anomalies. These findings refer to the compression of the thorax, cranial pushing of the diaphragm (decrease the space between the diaphragm and heart due to decrease of the ventral wall of CVC), and decrease of venous return (decrease the diameter of the CVC). These findings are somewhat mimic the findings which are associated with gastric dilatation and or volvulus in large and giant breed dogs (Kumar et al., 2024).

The findings of this study revealed that there were no substantial differences between the various structures observed in the left and right lateral radiographic views in each group, except for a few structures, such as CLA, CSA, trachea, and thoracic inlet. These results are largely consistent with those published in a previous study on goats (Abdelhakiem et

al., 2020). In the second group (non-anorectal group), the CLA appears shorter on the left lateral view compared to the right lateral view, with a P value of 0.019. This may be attributed to the less heart sternum contact on the left lateral view compared with the right lateral view (Thrall and Robertson, 2016). Interestingly, this finding was not observed in the anorectal group, which may be attributed to the compression of thoracic structures, including the heart, caused by abdominal distension and the cranial displacement of the diaphragm (Kumar et al., 2024).

The analysis of data from the current study showed that the CLA and CSA measurements are larger in the second group (non-anorectal) compared to those in the anorectal group. Conversely, the vertebral heart score (VHS) is significantly higher in the anorectal group, especially noted in the right lateral radiographic view, with a P value of 0.021 when compared to the non-anorectal group. The VHS is calculated as the sum of the CLA and CSA in relation to the number of thoracic vertebrae, starting from thoracic vertebra number 4 (Buchanan, 2000; Bodh et al., 2016; Thrall and Robertson, 2016; Bahr, 2018; Abdelhakiem et al., 2020). The decrease in the vertebral heart score (VHS), despite the increase in both cardiac short and long axes, may be attributed to the length of the thoracic vertebrae. If the bodies of the thoracic vertebrae are elongated, the VHS will decrease, and vice versa. Consequently, the authors believe that the VHS is not a reliable method for measuring cardiac size, as it does not accurately reflect the actual size of the heart. Fernández et al. (2023) reported that the vertebral heart size is affected in dogs by breed variations, and vertebral malformations. Bahr (2018) stated that the large variation of the measured VHS in different breeds of dogs (8.7- 10.7 vertebral unit) make the dependence of this score for evaluation of the cardiac size is considered inefficient. It is probably most useful in the same patient over time to compare cardiac size on serial radiographs. There are several methods used to measure heart size. One method involves comparing the width of the heart to the width of the thorax on ventrodorsal or dorsoventral views. Another method compares the length of the heart to the length of the thorax at the same level. The third method involves

Table 2. Differences between different thoracic structures in the two groups on the same lateral radiographic view

Thoracic structure	Right lateral view		Left lateral view	
	RLV anorectal	RLV others	LLV anorectal	LLV others
CLA (cm)	13.57± 0.27*	14.5± 0.34*	13.6± 0.22	14.21± 0.31
CSA (cm)	9.02± 0.26	9.69± 0.335	9.05± 0.3*	10.06± 0.36*
VHS (number of vertebrae)	9.6± 0.15*	9.04± 0.174*	9.5± 0.19	9.13± 0.19
Pulm. Artery (cm)	0.286± 0.0197	0.277± 0.0392	0.23± 0.033	0.25± 0.03
Pulm. Vein (cm)	0.285± 0.0193	0.2755± 0.0391	0.23± 0.032	0.26± 0.032
4th rib (cm)	0.56± 0.03	0.64± 0.04	0.56± 0.03*	0.65± 0.03*
Ratio 1	0.55± 0.05	0.45± 0.07	0.46± 0.07	0.39± 0.05
CVC (cm)	1.5± 0.135	1.81± 0.09	1.37± 0.112*	1.75± 0.105*
Aorta (cm)	1.88± 0.24	2.43± 0.27	1.66± 0.24	1.996± 0.42
Ratio 2	0.5± 0.072	0.62± 0.07	0.42± 0.76	0.48± 0.102
Sternum (number of sternebrae)	6.74± 0.1	6.64± 0.15	6.74± 0.1	6.64± 0.15
Trachea (cm)	1.16± 0.053	1.255± 0.057	1.14± 0.041*	1.33± 0.06*
Thoracic inlet (cm)	10.05± 0.185	10.291± 1.098	10.4± 0.24	11.19± 0.33
Ratio 3	0.12± 0.004	0.11± 0.004	0.10± 0.007	0.119± 0.006
Thoracic length (cm)	18.23± 0.31*	19.915± 0.43*	18.3± 0.35*	19.84± 0.383*
Thoracic axis (cm)	15.32± 1.3*	19.772± 0.66*	16.87± 0.61*	19.84± 0.62*
Ventral wall CVC (cm)	3.39± 0.3*	4.521± 0.33*	3.55± 0.35	4.17± 0.34
CLA/thoracic length	0.74± 0.008	0.73± 0.008	0.75± 0.009*	0.72± 0.009*
Frenendez method (CLA+CSA)/TIH	2.2± 0.0495	2.18± 0.0585	2.2± 0.0495	2.18± 0.059

Data are presented as Mean±SEM. The significant difference was superscripted by asterisk (*), which refers to the significant change in this thoracic structure between the two groups on the same lateral view.

CLA: cardiac long axis; CSA: cardiac short axis; VHS: vertebral heart score or scale; Pulm. Artery: pulmonary artery; pum. Vein: pulmonary vein; 4th rib: fourth rib; Ratio 1: pulm. Artery/4th rib; CVC: caudal vena cava; Ratio 2: CVC/Aorta; Ratio 3: trachea/thoracic inlet; ventral wall CVC: ventral wall of caudal vena cava; CLA/ thoracic length: cardiac long axis: thoracic length at the same point; CLA+ CSA/TIH: (cardiac long axis+ cardiac short axis)/ thoracic inlet height or length.

comparing the width of the heart to the number of intercostal spaces (Abdelhakiem *et al.*, 2020; Thrall and Robertson, 2016). There is a new published study in dogs which use the thoracic inlet for measurement of the cardiac size. The sum of CLA and CSA is divided by the thoracic inlet length. The authors stated that this method is feasible, reliable and reproducible (Fernández *et al.*, 2023). The authors of the present study used the Fernández's method for assessment of the cardiac size of the newly born calves in both groups. The findings revealed that there were no significant differences between the two groups or even in the same group between the RLV and LLV. From a clinical perspective, the author believes that the best method for assessing the size of the heart is a combination of patient history, clinical signs, and radiographic findings. The latter includes observing changes in the pulmonary blood vessels, aortic arch and the heart's outer contour through the use of the way of clock face analogy.

The present study found that there are 2 cranial pulmonary blood vessels which could be visualized and traced on the radiographs. The cranial pulmonary artery was dorsal to the vein and separated by bronchiole which appeared as a radiolucent channel without an obvious wall. This finding is consistent with what was published in goats (Abdelhakiem *et al.*, 2020). However, in dogs, the visualization of four cranial pulmonary vessels is achieved especially on the left lateral views (Thrall and Robertson, 2016).

The visualization of the cranial pulmonary blood vessels varied between the different views in the ano-rectal group. They were completely clear and obvious in all animals on the right lateral radiographic view, but they could not be detected in three animals out of nineteen on the left lateral radiographic view. This finding was not consistent with radiographic findings obtained in goats (Abdelhakiem *et al.*, 2020). They found that the cranial pulmonary blood vessels were fully detected on the left lateral radiographic projection. The visibility of the cranial pulmonary blood vessels on the left and right lateral views in the second group was equal. This might attribute the difference between the two views in the ano-rectal group to the abdominal distension resulting from the ano-rectal anomalies. The findings of the present study also revealed the lack of significant difference in the size of the cranial pulmonary artery and vein on the lateral radiographs in each group. This is in agreement with the data that was stated before (Losonsky *et al.*, 1983; Thrall and Robertson, 2016). However, they were inconsistent with radiographic findings which were recorded in goats (Abdelhakiem *et al.*, 2020). The study indicated that the CVC is more easily identified than the aorta in both views. This difference can be attributed to the anatomical locations of these structures and their relationships with surrounding tissues. The CVC is centrally positioned in the space between the heart and diaphragm, and its radiopaque properties contrast well against the radiolucent lung tissue, enhancing its visibility. In contrast, the aorta originates from the heart, passes close to the vertebrae, and then curves backward towards the diaphragm and abdomen. The upper portion of the aorta can be obscured by the ribs and vertebrae, which may hinder its detection and visualization, particularly in cases where the aorta is pushed upward.

The study also revealed the variation of the location of the tracheal bifurcation (carina) in calves. It is mainly detected at the level of C4-C5 in most cases on both views in the two groups. The Level of C5-C6 is considered the second level for detection of carina. These findings refers dynamics of the trachea which may be affected by the respiratory cycle (expiration and inspiration) or different external pressure (Wittenborg *et al.*, 1967).

The limitation of this study lies in the use of different animals for comparison. The radiographic findings of the thorax of animals with ano-rectal anomalies were compared to findings obtained from animals that did not have ano-rectal anomalies. Ideally, these findings should be evaluated within the same group of animals before and after surgical management. However, this was challenging for several reasons. Not all animals with ano-rectal anomalies underwent surgical management due to the owners' preferences. Furthermore, some animals unfortunately died

during the surgery. Also, after their surgical treatment, animals should return to the hospital for a radiographic examination a few days later. However, this has proven challenging because many owners are hesitant to bring their animals back due to the long distance to the hospital and the cost of transportation.

Conclusion

radiography proves to be an essential tool for understanding the thoracic anatomy of newborn calves. Ano-rectal anomalies result in significant alterations in certain thoracic structures due to abdominal distension and pressure on the diaphragm. Furthermore, various methods for evaluating cardiac size are considered unreliable and should not be exclusively relied upon for definitive conclusions regarding heart size.

Acknowledgments

The authors would like to thank Animal Surgery, Anesthesiology and Radiology Department, Faculty of Veterinary Medicine, Assiut University for approval of carrying out this study and their support.

Conflict of interest

The authors have no conflict of interest to declare.

References

- Abdelhakiem, M.A.H., 2020. Retrospective Study on the Unusual Clinical Presentations of Different Surgical Affections of the Digestive System in Large Ruminants. *J. Adv. Vet. Res.* 10, 29–40.
- Abdelhakiem, M.A.H., 2018. Sharp Foreign Body within the Thorax Concurrent with Pneumomediastinum in an Adult Cow: A Case Report. *J. Adv. Vet. Res.* 8, 101–103.
- Abdel-Hakiem, M.A.H., Aref, N., 2013. Prospective Study on AnoRectal Anomalies in Neonatal Farm Animals. *J. Vet. Adv.* 2, 595–604.
- Abdelhakiem, M.A.H., Khalphallah, A., Al-Iethie, A.A., 2020. Radiographic Appearance And Measurements Of Thoracic Structures Using Four Radiographic Projections In Goats. *Alex. J. Vet. Sci.* 64, 34–34. <https://doi.org/10.5455/ajvs.65920>
- Bahr, R.J., 2018. Textbook of Veterinary Diagnostic Radiology, 7th Edition | VetBooks [WWW Document]. URL <https://vetbooks.ir/textbook-of-veterinary-diagnostic-radiology-7th-edition/> (accessed 11.3.24).
- Berman, J., Masseur, I., Fecteau, G., Buczinski, S., Francoz, D., 2020. Comparison between thoracic ultrasonography and thoracic radiography for the detection of thoracic lesions in dairy calves using a two-stage Bayesian method. *Prev. Vet. Med.* 184, 105153. <https://doi.org/10.1016/j.prevetmed.2020.105153>
- Bodh, D., Hoque, M., Saxena, A.C., Guggoo, M.B., Bist, D., Chaudhary, J.K., 2016. Vertebral scale system to measure heart size in thoracic radiographs of Indian Spitz, Labrador retriever and Mongrel dogs. *Vet. World* 9, 371–376. <https://doi.org/10.14202/vetworld.2016.371-376>
- Buchanan, J.W., 2000. Vertebral scale system to measure heart size in radiographs. *Vet. Clin. North Am. Small Anim. Pract.* 30, 379–393.
- Carey, B., 1999. Neonatal Air Leaks: Pneumothorax, Pneumomediastinum, Pulmonary Interstitial Emphysema, Pneumopericardium. *Neonatal Netw.* 18, 81–84. <https://doi.org/10.1891/0730-0832.18.8.81>
- Farrow, C.S., 1999. Bovine Pneumonia: Its Radiographic Appearance. *Vet. Clin. North Am. Food Anim. Pract.* 15, 301–358. [https://doi.org/10.1016/S0749-0720\(15\)30184-5](https://doi.org/10.1016/S0749-0720(15)30184-5)
- Fernández, D.M., García, V., Santana, A.J., Montoya-Alonso, J.A., 2023. The Thoracic Inlet Heart Size, a New Approach to Radiographic Cardiac Measurement. *Anim. Open Access J. MDPI* 13, 389. <https://doi.org/10.3390/ani13030389>
- Kilic, N., Sarierler, M., 2004. Congenital intestinal atresia in calves: 61 Cases (1999-2003). *Rev. Médecine Vét.* 155, 381–384.
- Kumar, P., Surendran, S., Parathazhathayil, D., Kumar, J., Remya, V., 2024. Gastric dilatation and volvulus in dogs: a review of diagnosis, prevention, and treatment strategies. pp. 415–446.
- Losonsky, J.M., Thrall, D.E., Lewis, R.E., 1983. Thoracic Radiographic Abnormalities in 200 Dogs with Spontaneous Heartworm Infestation. *Vet. Radiol.* 24, 120–123. <https://doi.org/10.1111/j.1740-8261.1983.tb01550.x>
- Thrall, D.E., Robertson, I.D., 2016. Atlas of Normal Radiographic Anatomy & Anatomic Variants in the Dog and Cat. second. ed. Elsevier, 3251 Riverport Lane St. Louis, Missouri 63043.
- Wittenborg, M.H., Gyepes, M.T., Crocker, D., 1967. Tracheal Dynamics in Infants with Respiratory Distress, Stridor, and Collapsing Trachea. *Radiology* 88, 653–662. <https://doi.org/10.1148/88.4.653>